SIAM J. APPL. MATH.
Vol. 81, No. 6, pp. 2704–2724
© 2021 Society for Industrial and Applied Mathematics

Downloaded 01/30/25 to 108.147.175.114 . Redistribution subject to SIAM license or copyright; see https://epubs.siam.org/terms-privacy

CLASSICAL AND QUANTUM RANDOM-WALK CENTRALITY MEASURES IN MULTILAYER NETWORKS*

LUCAS BÖTTCHER† AND MASON A. PORTER‡

Abstract. Multilayer network analysis is a useful approach for studying networks of entities that interact with each other via multiple relationships. Classifying the importance of nodes and node-layer tuples is an important aspect of the study of multilayer networks. To do this, it is common to calculate various centrality measures, which allow one to rank nodes and node-layers according to a variety of structural features. In this paper, we formulate occupation, PageRank, betweenness, and closeness centralities in terms of node-occupation properties of different types of continuous-time classical and quantum random walks on multilayer networks. We apply our framework to a variety of synthetic and real-world multilayer networks, and we identify notable differences between classical and quantum centrality measures. Our computations give insights into the correlations between certain centralities that are based on random walks and associated centralities that are based on geodesic paths.

Key words. multilayer networks, centrality, classical random walks, quantum random walks

AMS subject classifications. 05C81, 68R10, 90C35, 81Q35

DOI. 10.1137/20M1385998

1. Introduction.

Centrality measures [4] are useful quantities to rank nodes in a network according to various notions of importance [36]. Depending on the centrality measure that one calculates, highly central nodes may be nodes with the most neighbors (degree centrality), ones that lie on many shortest paths between two nodes (geodesic betweenness centrality), ones that have a small distance (e.g., via a sum of shortest-path lengths) to many other nodes (closeness centrality), and so on. These and other centrality measures have a large variety of applications, including identifying important spreaders of diseases or information [29, 51], ranking websites and other things [15], and characterizing granular and particulate structures [34, 39].

A variety of centrality measures have been developed for monolayer networks and generalized to multilayer networks [3, 24, 56]. One prominent approach is to exploit the node-sampling properties of different types of classical random walks (CRWs) [12, 31, 37, 52, 53, 54]. Additionally, the study of quantum versions of CRWs called *continuous-time quantum walks* (CTQWs) [9, 45] has led to several insights into the influence of quantum effects on the propagation properties of random walks on networks. Quantum walks have been implemented in various experimental settings, including nuclear-magnetic-resonance setups [47], trapped neutral-atom systems [23] and trapped ion systems [49, 63], and photonic structures [7, 13, 42, 50]. One appealing property of quantum walks is that they can detect a "marked" (i.e., target) node quadratically faster than their classical counterparts on certain networks [9]. One can

*Received by the editors December 14, 2020; accepted for publication (in revised form) June 10, 2021; published electronically December 21, 2021.
https://doi.org/10.1137/20M1385998
Funding: The work of the first author was supported by the Swiss National Fund through grant P2EZP2-191888 and by the Army Research Office through grant W911NF-18-1-0345.
†Department of Computational Medicine, University of California, Los Angeles, CA 90095-1766 USA, and Computational Social Science, Frankfurt School of Finance and Management, Frankfurt am Main 60322, Germany (lucasb@g.ucla.edu).
‡Department of Mathematics, University of California, Los Angeles, CA 90095 USA and Santa Fe Institute, Santa Fe, NM 87501 USA (mason@math.ucla.edu).

Copyright © by SIAM. Unauthorized reproduction of this article is prohibited.

Downloaded 01/30/25 to 108.147.175.114 . Redistribution subject to SIAM license or copyright; see https://epubs.siam.org/terms-privacy

achieve full quantum speedup on many networks, including regular graphs [21], Erdős–Rényi (ER) networks [8], and d-dimensional cubic periodic lattices with $d \geq 5$ [9]. The advantage of quantum search strategies has been termed the "Grover speedup" in recognition of Lov Grover's foundational work on this topic [17, 18]. Recent studies [5, 30] have analyzed connections between the run times and success probabilities (where the success probability is the probability of finding a quantum walker at a target node at a certain time) of quantum search algorithms and the centralities of target nodes. For discrete-time quantum walks, it has been shown that success probability does not necessarily increase with closeness centrality [5]. However, for Cayley trees, the success probability is large for nodes with small "eccentricities" [30], where the eccentricity of a node is the maximum distance from it to any other node. A later study [43] illustrated that the run time of a CTQW-based search algorithm on a balanced binary tree is correlated with the closeness centrality of a preselected target node. Notably, all of these works computed centrality measures using classical algorithms. However, as described in [46, 48], it is also possible to define centrality measures that are based on the node-occupation statistics of quantum walks. Subsequently, numerical and experimental implementations of CTQW-based occupation centralities were compared to several classical centrality measures on random networks [19]. It has also been shown that one can tune node-occupation statistics of CRWs and CTQWs by using appropriate stochastic resetting protocols [59].

In the present paper, we build on ideas from [53] and compare several classical and quantum random-walk centrality measures on multilayer networks. Our paper proceeds as follows. In section 2, we give an overview of the standard mathematical formulation of multilayer networks. We then derive the evolution equations of CRWs and CTQWs on multilayer networks in section 3. In section 4, we use these evolution equations to define classical and quantum versions of random-walk occupation centrality, PageRank centrality, random-walk betweenness centrality, and random-walk closeness centrality. In section 5, we calculate these centrality measures for a variety of synthetic and empirical multilayer networks. We also examine correlations in two situations: (1) between random-walk and geodesic versions of betweenness centrality and (2) between random-walk and geodesic versions of closeness centrality. We conclude our study in section 6. Our source code (and additional information on parallelization methods) is publicly available at [6].

2. Multilayer networks. A graph (i.e., a monolayer network) $G = (V, E)$ is an ordered pair (V, E), where V is a set of N nodes and $E \subseteq V \times V$ is a set of edges that connect pairs of nodes. We label the nodes with the numbers $1, 2, \ldots, N$. For each node $v \in V$, the degree $\deg(v)$ is the number of edges that are attached to v.

To allow more than one layer in a network (see Figure 1), we use the multilayer-network formalism of [10, 24]. In addition to nodes and edges (as in a monolayer network), a multilayer network M has layers with d distinct aspects (i.e., types of layering, such as multiple types of relationships or multiple communication platforms) [44]. Each aspect a has a corresponding set L_a of *elementary layers*. We denote the sequence of sets of elementary layers by $L = \{L_a\}_{a=1}^{d}$. All possible combinations of elementary layers are given by the Cartesian product $L_1 \times \cdots \times L_d$, and elements of this set are called "layers." We denote the number of layers in M by K.

Not all nodes need to be present in all K layers. We use $V_M \subseteq V \times L$ to denote the set of node-layer tuples $(v, l) \in V_M$; node v, which represents some entity, is present in layer $l \subseteq L_1 \times \cdots \times L_d$. We denote the total number of nodes in M by $N = |V_M|$ and the subset of edges between node-layer tuples (i.e., "node-layers") by $E_M \subseteq V_M \times V_M$.

Copyright © by SIAM. Unauthorized reproduction of this article is prohibited.

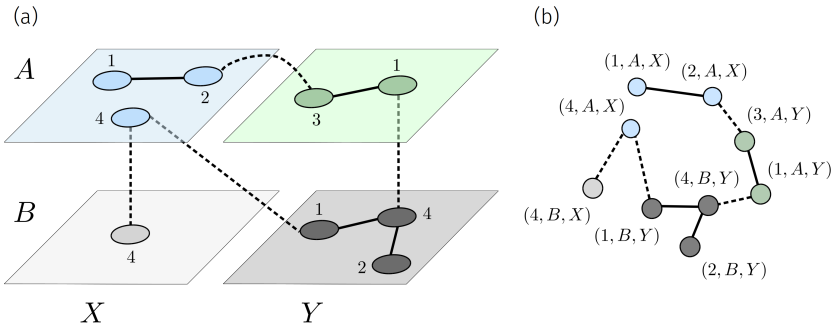

FIG. 1. Example of a multilayer network. (a) *We show a multilayer network* $M = (V_M, E_M, V, L)$ *with four nodes (i.e.,* $V = \{1, 2, 3, 4\}$*) and two aspects. These two aspects have corresponding elementary-layer sets* $L_1 = \{A, B\}$ *and* $L_2 = \{X, Y\}$*. The resulting four layers of* M *are* (A, X)*,* (A, Y)*,* (B, X)*, and* (B, Y)*. Not all nodes are present in all layers. In the depicted example, the set* V_M *of node-layer tuples is* $V_M = \{(1, A, X), (2, A, X), (4, A, X), (4, B, X), (1, A, Y), (3, A, Y), (1, B, Y), (2, B, Y), (4, B, Y)\} \subseteq V \times L_1 \times L_2$*.* (b) *The graph* $G_M = (V_M, E_M)$ *that corresponds to the multilayer network* M*. We indicate intralayer and interlayer edges using solid and dashed lines, respectively.*

The edge $((u, \alpha), (v, \beta)) \in E_M$ indicates that there is an edge from node u in layer α to node v in layer β (and vice versa, if M is undirected). Each aspect of M represents a type of layering, such as connections between (classical or quantum) circuits, a point in time, or some other property. We use the adjectives *intralayer* and *interlayer* to refer to edges between nodes in the same layer and between nodes in different layers, respectively. Using the above definitions, one can express a multilayer network (see Figure 1) as a quadruplet $M = (V_M, E_M, V, L)$ that consists of nodes (from the set V), node-layer tuples (from V_M), edges (from E_M), and layers (from L). A multiplex network is a specific type of multilayer network; in such a network, all of the interlayer edges occur between nodes and their counterparts in other layers.

3. Classical and quantum random walks. We consider an undirected and unweighted multilayer network M with adjacency tensor $\mathcal{A}$. The adjacency-tensor components are

$$\mathcal{A}_{j\beta}^{i\alpha} = \begin{cases} 1 & \text{if } (i, \alpha) \text{ is adjacent to } (j, \beta) \\ 0 & \text{otherwise}. \end{cases} \tag{3.1}$$

Note that $\mathcal{A}_{j\beta}^{i\alpha} = \mathcal{A}_{i\alpha}^{j\beta}$ for undirected networks. The transition probability of going from node i in layer α to node j in layer β is $T_{j\beta}^{i\alpha}$. To mathematically describe a CRW on M, let $p_{j\beta}(t)$ be the probability that a random walker is on node j in layer β in the time interval t. The corresponding temporal evolution of $p_{j\beta}(t)$ is

$$p_{j\beta}(t + \Delta t) = p_{j\beta}(t) - \Delta t \left[\sum_{(i,\alpha) \in V_M} T_{i\alpha}^{j\beta} p_{j\beta}(t) - \sum_{(i,\alpha) \in V_M} T_{j\beta}^{i\alpha} p_{i\alpha}(t) \right]. \tag{3.2}$$

As in the description of random-walk (and hence diffusion) dynamics on a monolayer network with the combinatorial graph Laplacian, we write $T_{j\beta}^{i\alpha} = \mathcal{A}_{j\beta}^{i\alpha} / k_{i\alpha}$, where $k_{i\alpha} = \sum_{(j,\beta) \in V_M} \mathcal{A}_{i\alpha}^{j\beta}$ is the degree of node i in layer α [22]. For brevity, we use the Einstein summation convention and write $k_{i\alpha} = \mathcal{A}_{i\alpha}^{j\beta} u_{j\beta}$, where all components of

Copyright © by SIAM. Unauthorized reproduction of this article is prohibited.

Downloaded 01/30/25 to 108.147.175.114 . Redistribution subject to SIAM license or copyright; see https://epubs.siam.org/terms-privacy

Downloaded 01/30/25 to 108.147.175.114 . Redistribution subject to SIAM license or copyright; see https://epubs.siam.org/terms-privacy

the covariant order-2 tensor $u_{j\beta}$ are equal to 1. Using the Einstein convention and $T^{i\alpha}_{j\beta} = \mathcal{A}^{i\alpha}_{j\beta}/k_{i\alpha}$, we rewrite (3.2) as

$$p_{j\beta}(t+\Delta t) = p_{j\beta}(t) - \Delta t \left[\delta^{i\alpha}_{j\beta} p_{i\alpha}(t) - \mathcal{A}^{k\gamma}_{j\beta} {D^{i\alpha}_{k\gamma}}^{-1} p_{i\alpha}(t)\right], \tag{3.3}$$

where the Kronecker delta $\delta^{i\alpha}_{j\beta} = 1$ if and only if $(i,\alpha) = (j,\beta)$ (so $\delta^{i\alpha}_{j\beta} = 0$ otherwise) and

$$D^{i\alpha}_{j\beta} = \begin{cases} k_{i\alpha} & \text{if } (i,\alpha) = (j,\beta) \\ 0 & \text{otherwise} \end{cases} \tag{3.4}$$

are the components of the degree tensor. In (3.3), we used the fact that

$$\sum_{(i,\alpha)\in V_M} T^{j\beta}_{i\alpha} = 1\,,$$

which indicates that the probability of going from node j in layer β to some other node-layer is 1 (because a random walker is required to move somewhere). This multilayer formulation of random-walk dynamics leads naturally to the definition of the components $L^{i\alpha}_{j\beta} = D^{i\alpha}_{j\beta} - \mathcal{A}^{i\alpha}_{j\beta}$ of the combinatorial Laplacian tensor [10].

For our analytical and numerical treatments of classical and quantum random walks on multilayer networks, we apply a *flattening* function [24,25] to the adjacency tensor and other tensors to transform them into associated $\mathcal{N}\times\mathcal{N}$ matrices with entries in $\mathbb{R}_{\geq 0}$. The scalar $\mathcal{N}$ denotes the number of nodes in $G_M = (V_M, E_M)$, which is the flattened graph representation of M. In our paper, we refer to the elements of V_M as "node-layers" because each node of $G_M = (V_M, E_M)$ is a node-layer of M. The supra-Laplacian matrix [16] $\mathbf{L}_{\mathrm{M}} = \mathbf{D}_{\mathrm{M}} - \mathbf{A}_{\mathrm{M}}$ allows us to write the evolution equation (3.3) in continuous time as

$$\frac{\mathrm{d}}{\mathrm{d}t}\mathbf{p} = -\mathcal{H}_{\mathrm{c}}\mathbf{p} \quad \text{with} \quad \mathcal{H}_{\mathrm{c}} = \mathbf{L}_{\mathrm{M}}\mathbf{D}_{\mathrm{M}}^{-1}\,. \tag{3.5}$$

The classical Hamiltonian $\mathcal{H}_{\mathrm{c}}$ is the generator of time translation of the flattened stochastic vector $\mathbf{p}$. Each component of $\mathbf{p}$ corresponds to a node-layer. In accordance with [14, 59], we use the normalized supra-Laplacian matrix $\hat{\mathbf{L}}_{\mathrm{M}} = \mathbf{D}_{\mathrm{M}}^{-1/2}\mathbf{L}_{\mathrm{M}}\mathbf{D}_{\mathrm{M}}^{-1/2}$ to formulate the evolution of a CTQW on multilayer networks according to the Schrödinger equation[1]

$$\frac{\mathrm{d}}{\mathrm{d}t}|\psi\rangle = -\mathrm{i}\mathcal{H}_{\mathrm{q}}|\psi\rangle \quad \text{with} \quad \mathcal{H}_{\mathrm{q}} = \hat{\mathbf{L}}_{\mathrm{M}}\,, \tag{3.6}$$

where $\mathrm{i} = \sqrt{-1}$. Because of the unitary and time-reversible evolution equation for CTQWs, these walks (unlike their classical counterparts) do not approach a stationary distribution. The stochastic nature of CTQWs comes from the measurement process rather than from the underlying dynamics [59]. A key advantage of CTQWs over their classical counterparts is that they are quadratically faster at detecting target nodes in certain networks [9]. This is a useful feature of centrality measures that are based on quantum walks.

[1] In this equation, we set $\hbar = 1$. Additionally, the choice of the quantum evolution operator is not unique. Following common choices for monolayer networks, appropriate choices of a Hermitian operator are the normalized supra-Laplacian matrix and the supra-adjacency matrix [61].

Copyright © by SIAM. Unauthorized reproduction of this article is prohibited.

Downloaded 01/30/25 to 108.147.175.114 . Redistribution subject to SIAM license or copyright; see https://epubs.siam.org/terms-privacy

4. Classical and quantum centralities.

4.1. Random-walk occupation centrality. For an undirected and connected multilayer network M, a CRW has a unique stationary state $\mathbf{p}^* \in \mathbb{R}^{\mathcal{N}}$ [38] that satisfies

$$\mathcal{H}_{\mathrm{c}}\mathbf{p}^* = 0 \quad \text{and} \quad \sum_{\tilde{i}=1}^{\mathcal{N}} p_{\tilde{i}}^* = 1\,, \tag{4.1}$$

where $\tilde{i}$ denotes a node-layer. We use a tilde to distinguish a node-layer $\tilde{i}$ of G_M from a node i of M. The solution of (4.1) is

$$p_{\tilde{i}}^* = \frac{k_{\tilde{i}}}{\sum_{\tilde{j}=1}^{\mathcal{N}} k_{\tilde{j}}}\,, \tag{4.2}$$

where $k_{\tilde{i}}$ is the (total) degree of node-layer $\tilde{i}$ in flattened notation (i.e., in the graph G_M). Each component of the stochastic vector $\mathbf{p}^*$ corresponds to the stationary CRW occupation probability (i.e., stationary density) of a certain node-layer and defines a natural random-walk centrality measure for a multilayer network. For CTQWs, however, unitary time evolution does not lead to a stationary state. Instead, the long-time behavior of a quantum walk is characterized by its long-time mean [14]

$$q_{\tilde{j}}^* = \lim_{T\to\infty} \frac{1}{T} \int_0^T \langle \tilde{j}|\rho(t)|\tilde{j}\rangle \,\mathrm{d}t\,, \tag{4.3}$$

where $\mathrm{d}t$ is an infinitesimal time step, $\rho(t) = |\psi(t)\rangle\langle\psi(t)|$ is a density operator, and $|\tilde{j}\rangle \in \mathbb{C}^{\mathcal{N}}$ is an orthonormal basis vector that satisfies

$$\langle \tilde{i}|\tilde{j}\rangle = \delta_{\tilde{i}\tilde{j}}\,. \tag{4.4}$$

Similarly to our notation for CRW occupation probability, $q_{\tilde{j}}^*$ denotes the CTQW occupation probability of node-layer $\tilde{j}$. Therefore, it gives a type of random-walk centrality.

4.2. PageRank centrality. We generalize the above definitions of random-walk occupation probabilities by incorporating teleportation events from (i,α) to (j,β) that occur with probability $1-a \in (0,1]$. In the classical setting, we replace the transition probability by

$$T_{j\beta}^{i\alpha} = a\mathcal{A}_{j\beta}^{i\alpha}/k_{i\alpha} + \frac{(1-a)}{NK} u_{j\beta}^{i\alpha} \tag{4.5}$$

for an undirected and connected multilayer network M [12, 53]. The order-4 tensor components $u_{j\beta}^{i\alpha}$ are equal to 1. In flattened notation, the resulting classical evolution equation is

$$\frac{\mathrm{d}}{\mathrm{d}t}\mathbf{p}_{\mathrm{p}} = -\mathcal{H}_{\mathrm{c}}^{\mathrm{p}}\mathbf{p}_{\mathrm{p}} \quad \text{with} \quad \mathcal{H}_{\mathrm{c}}^{\mathrm{p}} = a\mathbf{L}_{\mathrm{M}}\mathbf{D}_{\mathrm{M}}^{-1} + (1-a)\left[\mathbb{1} - \mathcal{N}^{-1}\mathbf{U}\right]\,, \tag{4.6}$$

where $\mathbf{U}$ is a matrix of 1 entries. The PageRank analog of (3.6) is

$$\frac{\mathrm{d}}{\mathrm{d}t}|\psi_{\mathrm{p}}\rangle = -\mathrm{i}\mathcal{H}_{\mathrm{q}}^{\mathrm{p}}|\psi_{\mathrm{p}}\rangle \quad \text{with} \quad \mathcal{H}_{\mathrm{q}}^{\mathrm{p}} = a\hat{\mathbf{L}}_{\mathrm{M}} + (1-a)\left[\mathbb{1} - \mathcal{N}^{-1}\mathbf{U}\right]\,. \tag{4.7}$$

Copyright © by SIAM. Unauthorized reproduction of this article is prohibited.

Downloaded 01/30/25 to 108.147.175.114 . Redistribution subject to SIAM license or copyright; see https://epubs.siam.org/terms-privacy

Note that $\mathcal{H}_{\mathrm{q}}^{\mathrm{p}}$ is Hermitian. In (4.6) and (4.7), we use a version of PageRank in which a random walker can teleport to any node-layer. Other teleportation protocols are also possible [15]. They lead to different PageRank Hamiltonians $\mathcal{H}_{\mathrm{c}}^{\mathrm{p}}$ and $\mathcal{H}_{\mathrm{q}}^{\mathrm{p}}$.

For different teleportation probabilities $1-a$, we calculate classical PageRank centrality by solving

$$\mathcal{H}_{\mathrm{c}}^{\mathrm{p}}\mathbf{p}_{\mathrm{p}}^{*}=0 \quad \text{and} \quad \sum_{\tilde{i}=1}^{\mathcal{N}}(\mathbf{p}_{\mathrm{p}}^{*})_{\tilde{i}}=1\,. \tag{4.8}$$

The associated quantum PageRank centrality is

$$(q_{\mathrm{p}}^{*})_{\tilde{j}}=\lim_{T\to\infty}\frac{1}{T}\int_{0}^{T}\langle\tilde{j}|\rho_{\mathrm{p}}(t)|\tilde{j}\rangle\,\mathrm{d}t\,, \tag{4.9}$$

where $\rho_{\mathrm{p}}(t)=|\psi_{\mathrm{p}}(t)\rangle\langle\psi_{\mathrm{p}}(t)|$. A discrete quantum-walk PageRank was proposed in [40], and CTQW and quantum-stochastic-walk (QSW) versions of PageRank were proposed in [28, 55].

4.3. Random-walk betweenness centrality. The betweenness centrality of a node quantifies the extent to which it lies on short paths that connect other nodes [36]. To formulate notions of betweenness centrality that are based on classical [35] and quantum random walks, we denote the transition-tensor components for a random walk with absorbing node ℓ in all layers by [53]

$$(T_{\ell})_{j\beta}^{i\alpha}=\begin{cases}0 & \text{if } i=\ell\\ T_{j\beta}^{i\alpha} & \text{if } i\neq\ell\,.\end{cases} \tag{4.10}$$

Because ℓ is an absorbing node, a random walk with transition-tensor components (4.10) stops after reaching node ℓ. Alternatively, one can define an absorbing transition tensor in terms of node-layer tuples (ℓ,γ) and corresponding transition probabilities $(T_{(\ell,\gamma)})_{j\beta}^{i\alpha}$ in a way that is analogous to (4.10).[2] Given $\mathcal{M}$ realizations of a classical or quantum random walk, the ensemble average of the number of times that a random walk that starts at node-layer (o,σ) with destination ℓ passes through (j,β) at time t is

$$(\tau_{\ell})_{j\beta}^{o\sigma}=\lim_{\mathcal{M}\to\infty}\frac{1}{\mathcal{M}}\sum_{m=1}^{\mathcal{M}}\int_{0}^{\infty}z_{j\beta}^{o\sigma}(t,m)\,\mathrm{d}t\,, \tag{4.11}$$

where $z_{j\beta}^{o\sigma}(t,m)\,\mathrm{d}t=1$ if the random-walk realization $m\in\{1,\dots,\mathcal{M}\}$ is at (j,β) in the time interval $[t,t+\mathrm{d}t)$ and $z_{j\beta}^{o\sigma}(t,m)\,\mathrm{d}t=0$ otherwise. Using

$$\bar{z}_{j\beta}^{o\sigma}(t)=\frac{1}{\mathcal{M}}\sum_{m=1}^{\mathcal{M}}z_{j\beta}^{o\sigma}(t,m) \tag{4.12}$$

yields

$$(\tau_{\ell})_{j\beta}^{o\sigma}=\int_{0}^{\infty}\bar{z}_{j\beta}^{o\sigma}(t)\,\mathrm{d}t\,. \tag{4.13}$$

[2]Centralities that are based on nodes and centralities that are based on node-layers are relevant for different problems. It is important to consider the scientific question that one is asking. For example, one can ask if a person is important on social media (and hence consider a node) or alternatively ask if a person has an important Twitter account (and hence consider a node-layer).

Copyright © by SIAM. Unauthorized reproduction of this article is prohibited.

Downloaded 01/30/25 to 108.147.175.114 . Redistribution subject to SIAM license or copyright; see https://epubs.siam.org/terms-privacy

Note that $(\tau_\ell)^{o\sigma}_{j\beta}$ diverges for $j = \ell$ because $\bar{z}^{o\sigma}_{j\beta} = 1$ after a walker reaches the absorbing node ℓ at some finite time.[3] Averaging over all possible starting layers σ and adding the number of times that a walk passes through node j in any of the K layers gives

$$(\tau_\ell)^o_j = \frac{1}{K}(\tau_\ell)^{o\sigma}_{j\beta} u^\beta u_\sigma \,, \tag{4.14}$$

where all components of the contravariant and covariant order-1 tensors u^β and u_σ are equal to 1. After averaging over all possible origins o and destinations ℓ, the random-walk betweenness centrality of node j is

$$\tau_j = \frac{1}{N(N-1)} \sum_{\ell=1}^{N} (\tau_\ell)^o_j u_o \,. \tag{4.15}$$

We now formulate CRW and quantum random-walk betweenness centralities. Let τ^{c}_j denote the CRW betweenness centrality of node j, and let τ^{q}_j denote the quantum random-walk betweenness centrality of node j. To determine the occupation probability $\bar{z}^{o\sigma}_{j\beta}(t)$ for CRW and CTQW dynamics with absorbing transition-tensor components $(T_\ell)^{i\alpha}_{j\beta}$, we modify the classical and quantum evolution equations (3.5) and (3.6). Reformulating (3.3) for an absorbing walk yields

$$\frac{\mathrm{d}}{\mathrm{d}t} p_{j\beta}(t) = - \begin{cases} -\mathcal{A}^{\ell\gamma}_{j\beta} {D^{i\alpha}_{\ell\gamma}}^{-1} p_{i\alpha}(t) & \text{if } j = \ell \text{ and } i \neq \ell \\ \delta^{i\alpha}_{j\beta} p_{i\alpha}(t) - \mathcal{A}^{\ell\gamma}_{j\beta} {D^{i\alpha}_{\ell\gamma}}^{-1} p_{i\alpha}(t) & \text{if } j \neq \ell \text{ and } i \neq \ell \\ 0^{i\alpha}_{j\beta} p_{i\alpha}(t) & \text{if } i = \ell \,, \end{cases} \tag{4.16}$$

where $0^{i\alpha}_{j\beta}$ is a tensor with entries that are equal to 0.

For our subsequent numerical calculations, we work in flattened notation and write the corresponding components of the classical absorbing-walk Hamiltonian with absorbing node-layer $\tilde{\ell}$ as

$$\big[(\mathcal{H}_{\tilde{\ell}})^{\mathrm{a}}_{\mathrm{c}}\big]_{\tilde{i}\tilde{j}} = \begin{cases} (\mathcal{H}_{\mathrm{c}})_{\tilde{i}\tilde{j}} & \text{if } \tilde{j} \neq \tilde{\ell} \\ 0 & \text{if } \tilde{j} = \tilde{\ell} \,. \end{cases} \tag{4.17}$$

Recall that, in flattened notation, the matrix element $-(\mathcal{H}_{\mathrm{c}})_{\tilde{i}\tilde{j}}$ (with $\tilde{i} \neq \tilde{j}$) describes the movement of a classical random walker from node-layer $\tilde{j}$ to node-layer $\tilde{i}$. We set $\big[(\mathcal{H}_{\tilde{\ell}})^{\mathrm{a}}_{\mathrm{c}}\big]_{\tilde{i}\tilde{j}} = 0$ for $\tilde{j} = \tilde{\ell}$ because a random walker that reaches an absorbing node-layer cannot leave it anymore.

Analogously to the classical absorbing-walk Hamiltonian (4.17), we write the quantum absorbing-walk Hamiltonian with absorbing node-layer $\tilde{\ell}$ as

$$\big[(\mathcal{H}_{\tilde{\ell}})^{\mathrm{a}}_{\mathrm{q}}\big]_{\tilde{i}\tilde{j}} = \begin{cases} (\mathcal{H}_{\mathrm{q}})_{\tilde{i}\tilde{j}} & \text{if } \tilde{j} \neq \tilde{\ell} \\ 0 & \text{if } \tilde{j} = \tilde{\ell} \,. \end{cases} \tag{4.18}$$

Because of the absorbing nature of this random walk, $(\mathcal{H}_{\tilde{\ell}})^{\mathrm{a}}_{\mathrm{q}}$ is not Hermitian. CTQWs with non-Hermitian Hamiltonians have been used as models of excitations that decay radiatively or via exciton recombination. See [32, 33, 62] for examples of applications of non-Hermitian Hamiltonians to systems with absorption. One application of such

[3] Such a singularity also occurs in the discrete-time formulation of random-walk betweenness centrality of [53], but this issue was not discussed in that paper.

Copyright © by SIAM. Unauthorized reproduction of this article is prohibited.

Downloaded 01/30/25 to 108.147.175.114 . Redistribution subject to SIAM license or copyright; see https://epubs.siam.org/terms-privacy

models is as a phenomenological description of how excitations in light-harvesting systems propagate until they become trapped in reaction centers (i.e., absorbing nodes) [62].

To determine the classical ($\boldsymbol{\tau}^{\mathrm{c}}$) and quantum ($\boldsymbol{\tau}^{\mathrm{q}}$) betweenness centralities using the Hamiltonians (4.17) (for the classical case) and (4.18) (for the quantum case), we employ a uniform walker distribution as an initial distribution for $\mathbf{p}(t)$ and $|\psi(t)\rangle$, respectively. Using a uniformly distributed initial walker configuration allows us to determine the evolution of absorbing CRWs and CTQWs for different initial node-layer configurations in parallel. This reduces the computational effort that is necessary to take a mean over all $\mathcal{N}$ initial walker positions. (See the summation over σ and o in (4.14) and (4.15).)

We now briefly summarize the steps that are necessary to compute the classical betweenness centrality $\boldsymbol{\tau}^{\mathrm{c}}$.

In flattened notation, we identify $\bar{z}$ with $e^{-(\mathcal{H}_{\tilde{\ell}})_{\mathrm{c}}^{\mathrm{a}}t}\mathbf{p}(0)$ and reformulate (4.13)–(4.15) as

$$\begin{aligned}\boldsymbol{\tau}^{\mathrm{c}} &= \lim_{s\to 0}\frac{1}{\mathcal{N}(\mathcal{N}-1)}\sum_{\tilde{\ell}}\int_0^\infty e^{-st}e^{-(\mathcal{H}_{\tilde{\ell}})_{\mathrm{c}}^{\mathrm{a}}t}\mathbf{p}(0)\,\mathrm{d}t \\ &= \lim_{s\to 0}\frac{1}{\mathcal{N}(\mathcal{N}-1)}\sum_{\tilde{\ell}}\left[s\mathbb{1}+(\mathcal{H}_{\tilde{\ell}})_{\mathrm{c}}^{\mathrm{a}}\right]^{-1}\mathbf{p}(0)\,,\end{aligned} \tag{4.19}$$

where we have inserted the prefactor e^{-st} (with $s>0$) because $(\mathcal{H}_{\tilde{\ell}})_{\mathrm{c}}^{\mathrm{a}}$ is a singular matrix and one cannot solve the integral in (4.13) in closed form for general networks. This formalism also avoids the divergence of the integral in (4.13) that arises from the presence of an absorbing state. The sum in (4.19) is over all node-layers $\tilde{\ell}$, and the integral over $e^{-st}e^{-(\mathcal{H}_{\tilde{\ell}})_{\mathrm{c}}^{\mathrm{a}}t}$ yields the resolvent $[s\mathbb{1}+(\mathcal{H}_{\tilde{\ell}})_{\mathrm{c}}^{\mathrm{a}}]^{-1}$ [41]. The discrete-time formulation of random-walk betweenness centrality in [53] results in an expression that is structurally similar to the continuous-time formulation of random-walk betweenness centrality in (4.19).

To calculate the quantum betweenness $\boldsymbol{\tau}^{\mathrm{q}}$, one needs to compute the node-occupation probabilities in (4.13) in terms of the squares of corresponding wavefunction entries. This yields

$$\tau_{\tilde{j}}^{\mathrm{q}} = \frac{1}{\mathcal{N}(\mathcal{N}-1)}\sum_{\tilde{\ell}}\int_0^\infty \langle\tilde{j}|\rho_{\tilde{\ell}}(t)|\tilde{j}\rangle\,\mathrm{d}t\,, \tag{4.20}$$

where $\rho_{\tilde{\ell}}(t)=|\psi_{\tilde{\ell}}(t)\rangle\langle\psi_{\tilde{\ell}}(t)|$ is the density matrix of the quantum absorbing walk with absorbing node-layer $\tilde{\ell}$. We use $|\psi_{\tilde{\ell}}(t)\rangle = e^{-\mathrm{i}(\mathcal{H}_{\tilde{\ell}})_{\mathrm{q}}^{\mathrm{a}}t}|\psi(0)\rangle$ and rewrite (4.20) as

$$\tau_{\tilde{j}}^{\mathrm{q}} = \frac{1}{\mathcal{N}(\mathcal{N}-1)}\sum_{\tilde{\ell}}\int_0^\infty\sum_{m,n} e^{-\mathrm{i}(\lambda_m^{(\tilde{\ell})}-\lambda_n^{(\tilde{\ell})})t}\langle e_m^{(\tilde{\ell})}|\psi(0)\rangle\langle\psi(0)|e_n^{(\tilde{\ell})}\rangle\langle\tilde{j}|e_m^{(\tilde{\ell})}\rangle\langle e_n^{(\tilde{\ell})}|\tilde{j}\rangle\,\mathrm{d}t\,, \tag{4.21}$$

where $e_m^{(\tilde{\ell})}$ and $\lambda_m^{(\tilde{\ell})}$, respectively, are the eigenvectors and corresponding eigenvalues of $(\mathcal{H}_{\tilde{\ell}})_{\mathrm{q}}^{\mathrm{a}}$. That is,

$$(\mathcal{H}_{\tilde{\ell}})_{\mathrm{q}}^{\mathrm{a}}e_m^{(\tilde{\ell})} = \lambda_m^{(\tilde{\ell})}e_m^{(\tilde{\ell})}\,. \tag{4.22}$$

The integral in (4.21) diverges if $\lambda_m^{(\tilde{\ell})}-\lambda_n^{(\tilde{\ell})}=0$. Therefore, as with CRW betweenness

Copyright © by SIAM. Unauthorized reproduction of this article is prohibited.

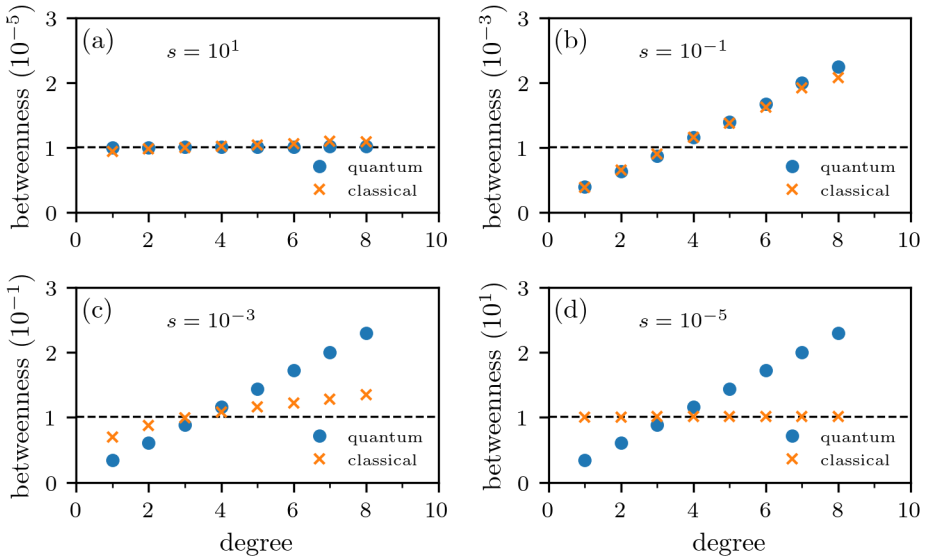

FIG. 2. Influence of the regularization parameter s on classical and quantum betweenness centralities. *We show classical (orange crosses) and quantum (blue disks) betweenness centralities for* (a) $s = 10^1$, (b) $s = 10^{-1}$, (c) $s = 10^{-3}$, *and* (d) $s = 10^{-5}$ *in* (4.19) *and* (4.23) *for a multilayer network with two Erdős–Rényi (ER) layers and* $N = 50$ *nodes in each layer. Interlayer edges connect each node-layer with its counterpart in the other layer. The expected mean degree in one layer is* 2, *and the expected mean degree in the other layer is* 3. *The dashed black line indicates the value* $[s\mathcal{N}(\mathcal{N}-1)]^{-1} \approx 10^{-4}/s$. *The product* $\mathcal{N}(\mathcal{N}-1)$ *is approximately* 10^{-4} *because the total number of node-layers in the multilayer network is* $\mathcal{N} = 100$. *As the initial condition, we use a uniform distribution over all node-layers. In this figure and in all subsequent figures, the numerical values along the vertical axes are multiplied by the number in parentheses (whenever there is one).*

centrality (4.19), we incorporate an additional prefactor e^{-st} (with $s > 0$) and obtain

$$\tau_{\tilde{j}}^{\mathrm{q}} = \lim_{s\to 0} \frac{1}{\mathcal{N}(\mathcal{N}-1)} \sum_{\tilde{\ell}} \sum_{m,n} \frac{\langle e_m^{(\tilde{\ell})}|\psi(0)\rangle \langle \psi(0)|e_n^{(\tilde{\ell})}\rangle}{s + \mathrm{i}(\lambda_m^{(\tilde{\ell})} - \lambda_n^{(\tilde{\ell})})} \langle \tilde{j}|e_m^{(\tilde{\ell})}\rangle \langle e_n^{(\tilde{\ell})}|\tilde{j}\rangle \ . \tag{4.23}$$

Observe the similarity in the mathematical structures of (4.21) and (4.23). In the quantum case (4.23), product states emerge as a result of mixing wavefunction components.

For our numerical calculations in section 5, we compute the classical (4.19) and quantum (4.23) random-walk betweenness centralities with a value of s that is small enough so that the "damping" term e^{-st} is not the dominant mechanism in the evolution of the classical and quantum absorbing random walks. As we detail in the next paragraph, the value of s also needs to be large enough so that classical walkers do not get trapped in absorbing states.

To study the influence of different values of s on continuous-time random-walk betweenness centrality, we calculate $\boldsymbol{\tau}^{\mathrm{c}}$ (see (4.19)) and $\boldsymbol{\tau}^{\mathrm{q}}$ (see (4.23)) for $s = 10^1$, $s = 10^{-1}$, $s = 10^{-3}$, and $s = 10^{-5}$ and a multilayer network with two $G(N,p)$ ER layers and $N = 50$ nodes in each layer (see Figure 2). The total number of node-layers is thus $\mathcal{N} = 100$. A layer's connection probability p determines the expected mean degree of that layer. As the initial condition for both the classical and quantum absorbing random walks, we use a uniform distribution over all node-layers. That is, $\mathbf{p}(0) = \mathcal{N}^{-1}(1,1,\ldots,1)^{\top}$ and $|\psi(0)\rangle = \mathcal{N}^{-1/2}(1,1,\ldots,1)^{\top}$. For these initial distri-

Copyright © by SIAM. Unauthorized reproduction of this article is prohibited.

Downloaded 01/30/25 to 108.147.175.114 . Redistribution subject to SIAM license or copyright; see https://epubs.siam.org/terms-privacy

Downloaded 01/30/25 to 108.147.175.114 . Redistribution subject to SIAM license or copyright; see https://epubs.siam.org/terms-privacy

butions and in the limit $s \to \infty$ (i.e., with "strong damping"), $\tau_{\tilde{j}}^{\mathrm{q}}$ and $\tau_{\tilde{j}}^{\mathrm{c}}$ approach $[s\mathcal{N}(\mathcal{N}-1)]^{-1}$ for each $\tilde{j}$. In Figure 2, we indicate this limiting value with a dashed black line. For $s = 10^{1}$, we observe that the values of classical and quantum betweenness centralities are very close to the limiting value (see Figure 2(a)). For $s = 10^{-1}$, the values of both centrality measures increase with the node degree (see Figure 2(b)). For progressively smaller values of s, CRW betweenness centrality again approaches the limiting value $[s\mathcal{N}(\mathcal{N}-1)]^{-1}$ (see Figure 2(c,d)) because the classical walks become trapped in absorbing states. For small values of s, quantum random-walk betweenness centrality is affected primarily by the magnitude of s because the mixing of the wavefunction components in (4.23) suppresses the effect of the absorbing states. As we illustrated in Figure 2, a value of $s = 10^{-1}$ is useful for calculating random-walk betweenness centrality. For the chosen initial conditions, substantially larger values of s yield strong damping. This leads to uniform node-occupation statistics in both the classical and the quantum random walks. If s is substantially smaller than 10^{-1}, the trapping of classical walks in absorbing states also leads to a uniform node-occupation distribution that one cannot use to distinguish between different nodes.

4.4. Random-walk closeness centrality. The closeness centrality of a node is based on the mean distance between that node and other nodes. One can compute some types of closeness centrality using absorbing random walks [36]. The probability that a random walker reaches the absorbing node ℓ at time $h \le t$ is [53]

$$(q_\ell)^{o\sigma}(h \le t) = u^{o\sigma} - \bar{z}^{o\sigma}_{j\beta}(t) u^{j\beta}\,, \tag{4.24}$$

where $\bar{z}^{o\sigma}_{j\beta}(t)$ is given by the expression in (4.12). The probability that the first-passage time (i.e., the time that a random walker takes to reach node ℓ) occurs in the interval $[t, t + \mathrm{d}t)$ is

$$\begin{aligned}
(q_\ell)^{o\sigma}(h = t)\mathrm{d}t &= \lim_{\Delta t \to 0} \left[(q_\ell)^{o\sigma}(h \le t + \Delta t) - (q_\ell)^{o\sigma}(h \le t)\right] \\
&= -\lim_{\Delta t \to 0} \left[\bar{z}^{o\sigma}_{j\beta}(t + \Delta t) u^{j\beta} - \bar{z}^{o\sigma}_{j\beta}(t) u^{j\beta}\right] \\
&= -\lim_{\Delta t \to 0} \left[\frac{\bar{z}^{o\sigma}_{j\beta}(t + \Delta t) - \bar{z}^{o\sigma}_{j\beta}(t)}{\Delta t}\right] u^{j\beta} \Delta t \\
&= -\bar{z}'^{o\sigma}_{j\beta}(t) u^{j\beta} \mathrm{d}t\,,
\end{aligned} \tag{4.25}$$

where $\bar{z}'^{o\sigma}_{j\beta}(t)$ is the derivative of $\bar{z}^{o\sigma}_{j\beta}(t)$ with respect to time. After determining $(q_\ell)^{o\sigma}(h = t)\mathrm{d}t$, we compute the mean first-passage time of a random walker that starts at node-layer (o, σ) and stops after reaching node ℓ in any layer. We obtain

$$\begin{aligned}
(H_\ell)^{o\sigma} &= \int_0^\infty t (q_\ell)^{o\sigma}(h = t)\, \mathrm{d}t = -\int_0^\infty t \bar{z}'^{o\sigma}_{j\beta}(t) u^{j\beta} \mathrm{d}t \\
&= -t \bar{z}^{o\sigma}_{j\beta}(t) u^{j\beta}\big|_0^\infty + \int_0^\infty \bar{z}^{o\sigma}_{j\beta}(t) u^{j\beta} \mathrm{d}t \\
&= -\lim_{t \to \infty} t \bar{z}^{o\sigma}_{j\beta}(t) u^{j\beta} + \int_0^\infty \bar{z}^{o\sigma}_{j\beta}(t) u^{j\beta} \mathrm{d}t \\
&= (\tau_\ell)^{o\sigma}_{j\beta} u^{j\beta}\,.
\end{aligned} \tag{4.26}$$

In the last equality, we used the fact that $\bar{z}^{o\sigma}_{j\beta}(t)$ vanishes for long times because every walker is eventually absorbed by node ℓ. Consequently, the mean first-passage time $(H_\ell)^{o\sigma}$ is equal to $(\tau_\ell)^{o\sigma}_{j\beta} u^{j\beta}$ and is thus related to random-walk betweenness centrality

Copyright © by SIAM. Unauthorized reproduction of this article is prohibited.

Downloaded 01/30/25 to 108.147.175.114 . Redistribution subject to SIAM license or copyright; see https://epubs.siam.org/terms-privacy

(see (4.13)). For discrete-time CRWs, an analogous relationship between the mean first-passage time and random-walk betweenness centrality was derived in [53].

Averaging over $(H_\ell)^{o\sigma}$ for all nodes and layers yields the mean first-passage time

$$\begin{aligned} h_\ell &= \frac{1}{(N-1)K}(H_\ell)^{o\sigma}u_{o\sigma} + \frac{1}{N}\pi_\ell^{-1} \\ &= \frac{1}{(N-1)K}(\tau_\ell)^{o\sigma}_{j\beta}u^{j\beta}u_{o\sigma} + \frac{1}{N}\pi_\ell^{-1}\,, \end{aligned} \tag{4.27}$$

where π_ℓ is the (classical or quantum) random-walk occupation probability of node ℓ. Because of the absorbing nature of the random walk that underlies the definition of $(\tau_\ell)^{o\sigma}_{j\beta}$, we explicitly include the mean return time π_ℓ^{-1} in (4.27). The random-walk closeness centrality of node ℓ is $1/h_\ell$. Equation (4.27) thus connects closeness, betweenness, and occupation centralities.

As with random-walk betweenness centrality, the random-walk closeness centrality h_ℓ^{-1} is based on the occupation probability $\bar{z}^{o\sigma}_{j\beta}(t)$ of an absorbing random walk. We proceed as in section 4.3 and compute this probability, in flattened notation, using (4.13), (4.19), and (4.23). We write

$$h_{\tilde{\ell}} = \frac{1}{\mathcal{N}-1}(\tau_{\tilde{\ell}})^{\tilde{o}}_{\tilde{j}}u^{\tilde{j}}u_{\tilde{o}} + \frac{1}{\mathcal{N}}\pi_{\tilde{\ell}}^{-1}\,. \tag{4.28}$$

In flattened notation, $\pi_{\tilde{\ell}}$ is given by $p^*_{\tilde{\ell}}$ in the classical case (see (4.8)) and $q^*_{\tilde{\ell}}$ in the quantum case (see (4.3)). In Table 1, we summarize the classical and quantum multilayer random-walk centrality measures that we have discussed.

5. Numerical examples. In this section, we present some numerical examples of the random-walk centrality measures from section 4. See Table 1 for a summary of these centralities. We compare these classical and quantum random-walk centralities for two types of synthetic and empirical multilayer networks. In our numerical examples (and when it is convenient for clarity), we often use the term "node" both for the entities in a network and for their associated node-layers.

Our first example of a synthetic multilayer network consists of two $G(N,p)$ ER layers with $N = 1000$ nodes each and $p = 0.04$ and $p = 0.06$, respectively. The expected mean degree of one layer is 40, and the expected mean degree of the other layer is 60. Our second synthetic multilayer network consists of one $G(N,p)$ ER layer with $p = 0.04$ and one Barabási–Albert (BA) layer. The former has an expected mean degree of 40. To construct the latter, we start with two isolated nodes and iteratively add new nodes until there are $N = 1000$ nodes. Each new node has 2 edges that connect to existing nodes using linear preferential attachment [36]. Both layers have $N = 1000$ nodes. In both of these examples, each node-layer is adjacent to its counterpart in the other layer but not to any other node-layers in the other layer. Consequently, both synthetic multilayer networks are multiplex networks (see section 2).

We also calculate centralities for two empirical multilayer networks. The first one is the Lazega Law Firm network [1, 27], which has 71 nodes and 2571 edges. It has three different edge types, which encode different relationships between partners and associates of a corporate law firm. The second empirical multilayer network is the London metropolitan ("Tube") network [2, 11], which has 369 nodes and 441 edges. It also has three edge types, which encode connections within the three layers (Underground, Overground, and Docklands Light Railway) of London metro stations. As in the synthetic networks, in each of these examples, each node-layer is adjacent to its counterpart in the other layer (and not to any other node-layers in the other layer).

Copyright © by SIAM. Unauthorized reproduction of this article is prohibited.

Downloaded 01/30/25 to 108.147.175.114 . Redistribution subject to SIAM license or copyright; see https://epubs.siam.org/terms-privacy

TABLE 1

Definitions of several classical and quantum multilayer random-walk centrality measures. *We summarize the employed definitions of classical and quantum random-walk occupation, PageRank, random-walk betweenness, and random-walk closeness centralities. The CRW Hamiltonian is the product of the combinatorial supra-Laplacian matrix* $\mathbf{L}_{\mathrm{M}}$ *and the inverse-degree supramatrix* $\mathbf{D}_{\mathrm{M}}^{-1}$*. For the CTQW, we use the normalized supra-Laplacian matrix* $\hat{\mathbf{L}}_{\mathrm{M}}$*. The identity matrix is* $\mathbb{1}$*, and* $\mathbf{U}$ *is the matrix of* 1 *entries. We present all centralities in flattened multilayer notation. (In such notation, each element of a vector corresponds to a node-layer.) The number of node-layers is* $\mathcal{N}$*. We use* $u^{\tilde{\jmath}}$ *and* $u_{\tilde{o}}$*, respectively, to denote the components of the contravariant and covariant order-*1 *tensors in which all entries are equal to* 1*.*

Centrality	Classical	Quantum
occupation	$\mathbf{p}^*$, which is the stationary state of $\frac{\mathrm{d}}{\mathrm{d}t}\mathbf{p} = -\mathcal{H}_{\mathrm{c}}\mathbf{p}$ with the CRW Hamiltonian $\mathcal{H}_{\mathrm{c}} = \mathbf{L}_{\mathrm{M}}\mathbf{D}_{\mathrm{M}}^{-1}$	$\mathbf{q}^*$, which is the long-time mean (4.3) of the components of the density matrix $\rho(t) = \lvert\psi(t)\rangle\langle\psi(t)\rvert$ with $\frac{\mathrm{d}}{\mathrm{d}t}\lvert\psi\rangle = -\mathrm{i}\mathcal{H}_{\mathrm{q}}\lvert\psi\rangle$ and the CTQW Hamiltonian $\mathcal{H}_{\mathrm{q}} = \hat{\mathbf{L}}_{\mathrm{M}}$
PageRank	$\mathbf{p}_{\mathrm{p}}^*$, which is based on the PageRank Hamiltonian $\mathcal{H}_{\mathrm{c}}^{\mathrm{p}} = a\mathcal{H}_{\mathrm{c}} + (1-a)(\mathbb{1} - \mathcal{N}^{-1}\mathbf{U})$ with teleportation probability $1-a$	$\mathbf{q}_{\mathrm{p}}^*$, which is based on the PageRank Hamiltonian $\mathcal{H}_{\mathrm{c}}^{\mathrm{q}} = a\mathcal{H}_{\mathrm{q}} + (1-a)(\mathbb{1} - \mathcal{N}^{-1}\mathbf{U})$ with teleportation probability $1-a$
betweenness	$\boldsymbol{\tau}^{\mathrm{c}} \propto \lim_{s\to 0}\sum_{\tilde{\ell}}\left[s\mathbb{1} + (\mathcal{H}_{\tilde{\ell}})_{\mathrm{c}}^{\mathrm{a}}\right]^{-1}\mathbf{p}(0)$, where $(\mathcal{H}_{\tilde{\ell}})_{\mathrm{c}}^{\mathrm{a}}$ is the classical absorbing-walk Hamiltonian (4.17) with absorbing node-layer $\tilde{\ell}$	$\tau_{\tilde{\jmath}}^{\mathrm{q}} \propto \lim_{s\to 0}\sum_{\tilde{\ell}}\sum_{m,n}\frac{\langle e_m^{(\tilde{\ell})}\lvert\psi(0)\rangle\langle\psi(0)\rvert e_n^{(\tilde{\ell})}\rangle}{s+\mathrm{i}(\lambda_m^{(\tilde{\ell})}-\lambda_n^{(\tilde{\ell})})}\langle\tilde{\jmath}\rvert e_m^{(\tilde{\ell})}\rangle\langle e_n^{(\tilde{\ell})}\rvert\tilde{\jmath}\rangle$, where $e_m^{(\tilde{\ell})}$ and $\lambda_m^{(\tilde{\ell})}$, respectively, are the eigenvectors and eigenvalues of the quantum absorbing-walk Hamiltonian (4.18) with absorbing node-layer $\tilde{\ell}$
closeness	$(h_{\tilde{\ell}}^{\mathrm{c}})^{-1}$, where $h_{\tilde{\ell}}^{\mathrm{c}} = \frac{1}{\mathcal{N}-1}(\tau_{\tilde{\ell}}^{\mathrm{c}})_{\tilde{\jmath}}^{\tilde{o}}u^{\tilde{\jmath}}u_{\tilde{o}} + \frac{1}{\mathcal{N}}{p_{\tilde{\ell}}^*}^{-1}$ is the mean first-passage time	$(h_{\tilde{\ell}}^{\mathrm{q}})^{-1}$, where $h_{\tilde{\ell}}^{\mathrm{q}} = \frac{1}{\mathcal{N}-1}(\tau_{\tilde{\ell}}^{\mathrm{q}})_{\tilde{\jmath}}^{\tilde{o}}u^{\tilde{\jmath}}u_{\tilde{o}} + \frac{1}{\mathcal{N}}{q_{\tilde{\ell}}^*}^{-1}$ is the mean first-passage time

Copyright © by SIAM. Unauthorized reproduction of this article is prohibited.

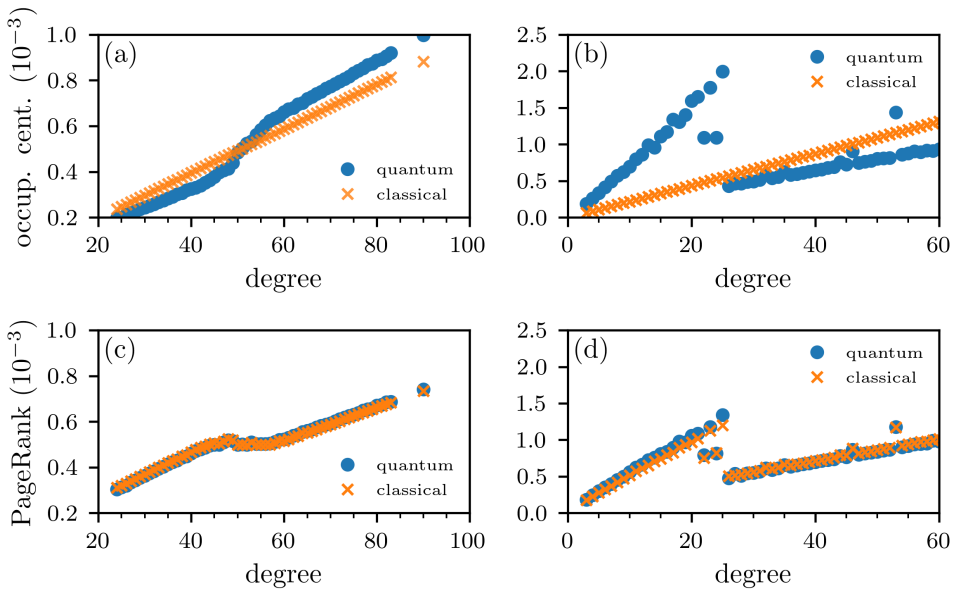

FIG. 3. Classical and quantum occupation centrality and PageRank centrality on synthetic multilayer networks. *We show classical (orange crosses) and quantum (blue disks) random-walk centralities (with occupation centrality in panels* (a,b) *and PageRank centrality with* $a = 0.85$ *in panels* (c,d)*) for two multilayer networks with two layers and* $N = 1000$ *nodes in each layer.* (a,c) *The multilayer network consists of two ER layers and interlayer edges that connect each node-layer with its counterpart in the other layer. The expected mean degree in one layer is* 40*, and the expected mean degree in the other layer is* 60. (b,d) *The multilayer network consists of one ER layer and one BA layer. Interlayer edges connect each node-layer with its counterpart in the other layer. The expected mean degree of the ER layer is* 40*. In the BA layer, we start with two isolated nodes and iteratively add new nodes until there are* $N = 1000$ *nodes. Each new node has* 2 *edges that connect to existing nodes using linear preferential attachment. As the initial condition for each calculation, we use a uniform distribution over all node-layers.*

To illustrate the results of our calculations, we plot node-layer centralities versus node-layer degrees. In Figure 3(a,b), we show our results for classical and quantum random-walk occupation centralities on our synthetic multilayer networks. The linear dependence of the classical occupation centrality on node-layer degree that we observe in our numerical results is explained by equation (4.2). Unlike classical walks, quantum walks do not approach a stationary state and do not satisfy (4.2). Instead, their long-time behavior is characterized by the long-time mean (4.3). Our results in Figure 3(a,b) suggest that the node-layer occupation properties of CTQWs are not captured by node-layer degree alone (so, in particular, they are not proportional to node-layer degree). These properties also depend on other structural features of the networks. The minimum and maximum degrees of the BA layer of the multilayer network in Figure 3(b,d) are 2 and 52, respectively. In the network's ER layer, the minimum and maximum degrees are 21 and 60, respectively. In Figure 3(d), we observe that some of the node-layers (specifically, those with degrees that are smaller than 21) in the BA layer have larger classical and quantum PageRank centralities than some of the node-layers in the ER layer. These differences are associated with the deviations from monotonic behavior of classical occupation centrality that we observe in Figure 3(b).

In our two synthetic multilayer networks, we observe more pronounced differences between classical and quantum occupation centralities than was the case for the

Copyright © by SIAM. Unauthorized reproduction of this article is prohibited.

Downloaded 01/30/25 to 108.147.175.114 . Redistribution subject to SIAM license or copyright; see https://epubs.siam.org/terms-privacy

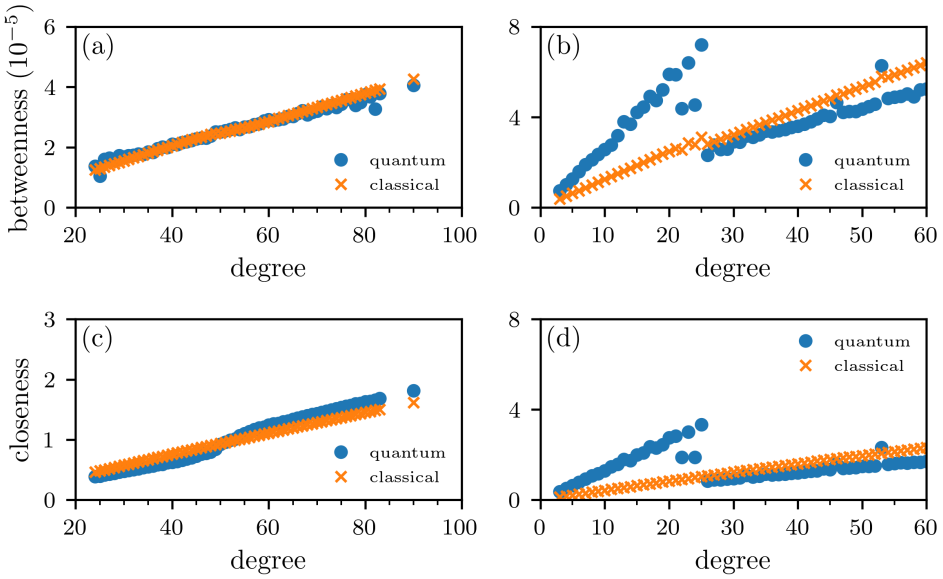

FIG. 4. Classical and quantum random-walk betweenness centrality and random-walk closeness centrality on synthetic multilayer networks. *We show classical (orange crosses) and quantum (blue disks) random-walk centralities (with betweenness centrality in panels* (a,b) *and closeness centrality in panels* (c,d)*) for two multilayer networks with two layers and* $N = 1000$ *nodes in each layer. In the resolvent (see Table* 1*), we set* $s = 0.01$. (a,c) *The multilayer network consists of two ER layers and interlayer edges that connect each node-layer with its counterpart in the other layer. The expected mean degree in one layer is* 40*, and the expected mean degree in the other layer is* 60. (b,d) *The multilayer network consists of one ER layer and one BA layer. Interlayer edges connect each node-layer with its counterpart in the other layer. The expected mean degree of the ER layer is* 40*. In the BA layer, we start with two isolated nodes and iteratively add new nodes until there are* $N = 1000$ *nodes. Each new node has* 2 *edges that connect to existing nodes using linear preferential attachment. As the initial condition for each calculation, we use a uniform distribution over all node-layers.*

monolayer ER and BA networks that were studied in [14]. Additionally, we observe that the differences between these two formulations of occupation centrality are larger in the synthetic multilayer network that includes a BA layer than in the network that consists of two ER layers. This arises from the large degree heterogeneity in the BA layer [14].

In Figure 3(c,d), we show the occupation probabilities for classical and quantum PageRank with a teleportation probability of $1-a = 0.15$. The classical and quantum occupation statistics are almost identical, which differs starkly from our observations for occupation centrality in Figure 3(a,b). This observation suggests that nonzero teleportation probabilities counteract differences in the node-occupation statistics between classical and quantum walks. In the limit $a \to 0$ (in which there is teleportation dynamics only), classical and quantum PageRank yield the same occupation statistics because all nodes are occupied with the same probability.

To further compare the classical and quantum random-walk centralities on multilayer networks, we also compute random-walk betweenness and random-walk closeness for our two synthetic multilayer networks. In Figure 4(a,b), we show our results for betweenness centrality and observe notable differences in our two synthetic multilayer networks. For the multilayer network with a BA layer, the quantum random-walk betweennesses of small-degree nodes is larger than their CRW betweennesses. The

Copyright © by SIAM. Unauthorized reproduction of this article is prohibited.

Downloaded 01/30/25 to 108.147.175.114 . Redistribution subject to SIAM license or copyright; see https://epubs.siam.org/terms-privacy

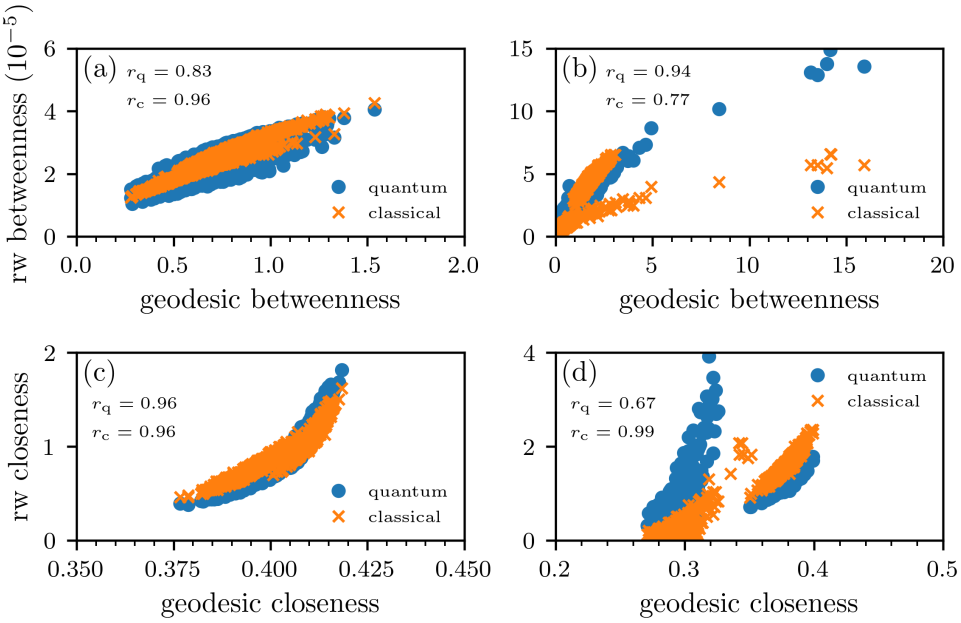

FIG. 5. Correlations between random-walk and geodesic centralities on synthetic multilayer networks. *We show the correlations between random-walk ("rw") and geodesic betweenness seness on two multilayer networks with two layers and* $N = 1000$ *nodes in each layer. We use* r_c *and* r_q *to denote the numerical values of the Pearson correlation coefficients for classical and quantum centralities, respectively. We indicate the classical and quantum random-walk centralities using orange crosses and blue disks, respectively. In the resolvent (see Table* 1*), we set* $s = 0.01$. (a,c) *The multilayer network consists of two ER layers with interlayer edges that connect each node-layer with its counterpart in the other layer. The expected mean degree in one layer is* 40*, and the expected mean degree in the other layer is* 60. (b,d) *The multilayer network consists of one ER layer and one BA layer. Interlayer edges connect each node-layer with its counterpart in the other layer. The expected mean degree of the ER layer is* 40*. In the BA layer, we start with two isolated nodes and iteratively add new nodes until there are* $N = 1000$ *nodes. Each new node has* 2 *edges that connect to existing nodes using linear preferential attachment. As the initial condition for each calculation, we use a uniform distribution over all node-layers.*

opposite holds for most nodes with degrees that are at least 26 (see Figure 4(b)). Our computation of closeness centralities in Figure 4(c,d) illustrates that classical and quantum random-walk closeness centralities quantify node-layer importance in the examined networks in a way that is similar to occupation centrality (see Figure 3(a,b)). This observation is intuitive because occupation centrality appears in the definition (4.28) of random-walk closeness centrality. One can also calculate betweenness and closeness centralities that are based on shortest paths instead of on random walks. Such geodesic centrality measures give an alternative notion of betweenness and closeness in networks. In Figure 5, we show the correlations between the random-walk and geodesic versions of these centralities for our synthetic multilayer networks. We observe that the random-walk and geodesic centralities are positively correlated with each other. For the multilayer network with two ER layers, the Pearson correlation coefficients are 0.96 (classical) and 0.83 (quantum) for betweenness centrality and 0.96 (classical) and 0.96 (quantum) for closeness centrality. For the multilayer network with an ER layer and a BA layer, the Pearson correlation coefficients are 0.77 (classical) and 0.94 (quantum) for betweenness centrality and 0.99

Downloaded 01/30/25 to 108.147.175.114 . Redistribution subject to SIAM license or copyright; see https://epubs.siam.org/terms-privacy

Copyright © by SIAM. Unauthorized reproduction of this article is prohibited.

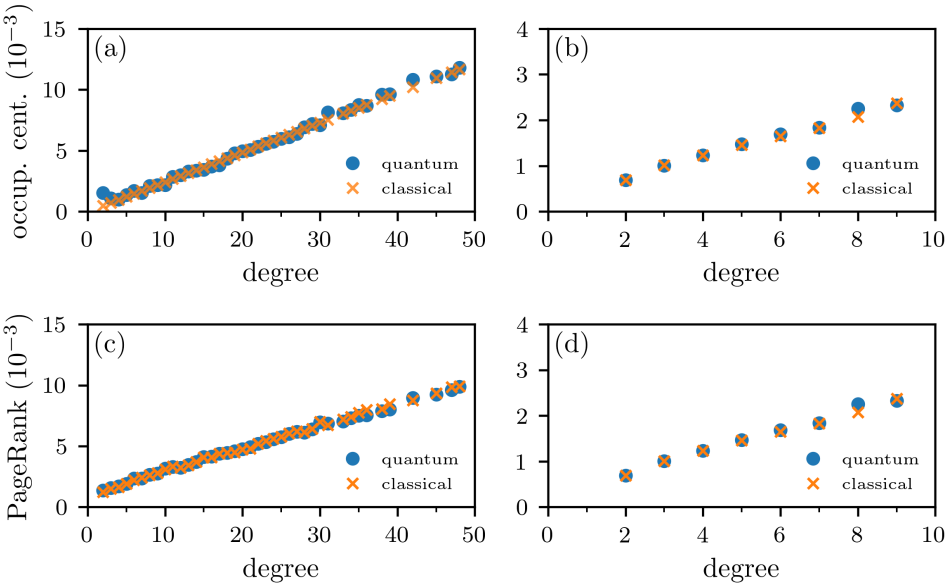

FIG. 6. Classical and quantum occupation centrality and PageRank centrality on empirical multilayer networks. *We show classical (orange crosses) and quantum (blue disks) random-walk centralities (with occupation centrality in panels* (a,b) *and PageRank centrality for* $a = 0.85$ *in panels* (c,d)*) for two empirical multilayer networks.* (a,c) *The Lazega Law Firm network, which has* 71 *nodes and* 2571 *edges. It has three edge types, which represent different relationships between partners and associates of a corporate law firm.* (b,d) *A multilayer network of the London metropolitan ("Tube") transportation network, which has* 369 *nodes and* 441 *edges. It has three edge types, which encode connections within the three layers (Underground, Overground, and Docklands Light Railway) of London metro stations. In both multilayer networks, interlayer edges connect each node-layer with its counterpart in the other layer. As the initial condition for each calculation, we use a uniform distribution over all node-layers.*

(classical) and 0.67 (quantum) for closeness centrality. The p-values for all correlation coefficients are smaller than (single) machine precision.

We now calculate classical and quantum occupation, PageRank, betweenness, and closeness centralities for our two empirical networks. In Figure 6, we show the results of our numerical calculations of occupation and PageRank centralities and observe that the differences between these classical and quantum centralities are smaller than those that we observed for the synthetic multilayer networks in Figure 3. Similarly, the differences between classical and quantum betweenness and closeness centralities that we show in Figure 7 are smaller than those that we observed for the synthetic multilayer networks in Figure 4.

As with our two synthetic multilayer networks, we examine the correlations between geodesic betweenness and closeness and their random-walk counterparts (see Figure 8). For the Lazega Law Firm network, the Pearson correlation coefficients are 0.87 (classical) and 0.85 (quantum) for betweenness centrality and 0.95 (classical) and 0.92 (quantum) for closeness centrality. For the London Tube transportation network, the Pearson correlation coefficients are 0.74 (classical) and 0.74 (quantum) for betweenness centrality and 0.21 (classical) and 0.21 (quantum) for closeness centrality. The p-values for all correlation coefficients are smaller than (single) machine precision.

We find that the large differences between classical and quantum random-walk occupation centrality are associated with a large degree heterogeneity in the layers of

Downloaded 01/30/25 to 108.147.175.114 . Redistribution subject to SIAM license or copyright; see https://epubs.siam.org/terms-privacy

Copyright © by SIAM. Unauthorized reproduction of this article is prohibited.

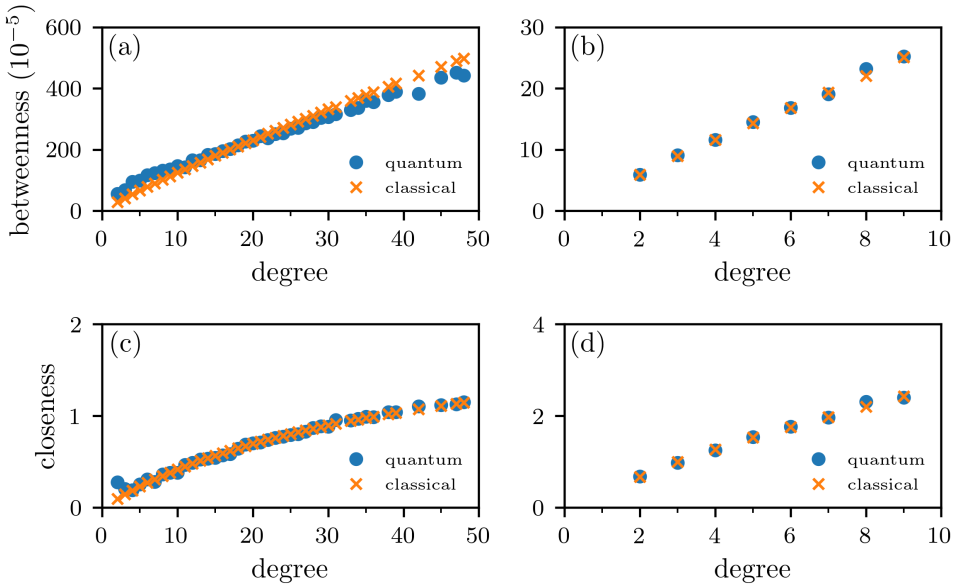

FIG. 7. Classical and quantum random-walk betweenness and random-walk closeness on empirical multilayer networks. *We show the classical (orange crosses) and quantum (blue disks) random-walk centralities (with betweenness centrality in panels* (a,b) *and closeness centrality in panels* (c,d)*) for two empirical multilayer networks. In the resolvent (see Table* 1*), we set* $s = 0.01$. (a,c) *The Lazega Law Firm network, which has* 71 *nodes and* 2571 *edges. It has three edge types, which encode different relationships between partners and associates of a corporate law firm.* (b,d) *A multilayer network of the London metropolitan ("Tube") network, which has* 369 *nodes and* 441 *edges. It has three edge types, which encode connections within the three layers (Underground, Overground, and Docklands Light Railway) of London metro stations. In both multilayer networks, interlayer edges connect each node-layer with its counterpart in the other layer. As the initial condition for each calculation, we use a uniform distribution over all node-layers.*

the examined networks. These observations are similar to the results in [14]. However, our results for the multilayer network with a BA layer contrast starkly with those of which we are aware. Specifically, the difference between classical and quantum random-walk occupation centrality in this synthetic multilayer network is significantly larger than those that were reported for monolayer networks in [14, 59].

6. Conclusions and discussion. We formulated and analyzed classical and quantum continuous-time random-walk centrality measures in multilayer networks. We have three main contributions. First, we generalized the classical discrete-time random-walk centralities of [53] to continuous time. Second, we introduced and studied continuous-time quantum-walk generalizations of occupation, PageRank, betweenness, and closeness centralities. Third, we formulated continuous-time classical and quantum centrality measures for both monolayer and multilayer networks. Our results complement earlier studies that focused on quantum occupation [19, 46, 48, 59] and PageRank [28, 55] centrality measures on monolayer networks.

In continuous time, the evolution of the underlying classical and quantum walks is described by different Hamiltonians, which we summarized in Table 1. One can derive other classical and quantum continous-time random-walk centralities by modifying these Hamiltonians and tracking different properties of absorbing random walks, which are what we used to define random-walk betweenness and closeness.

Downloaded 01/30/25 to 108.147.175.114 . Redistribution subject to SIAM license or copyright; see https://epubs.siam.org/terms-privacy

Copyright © by SIAM. Unauthorized reproduction of this article is prohibited.

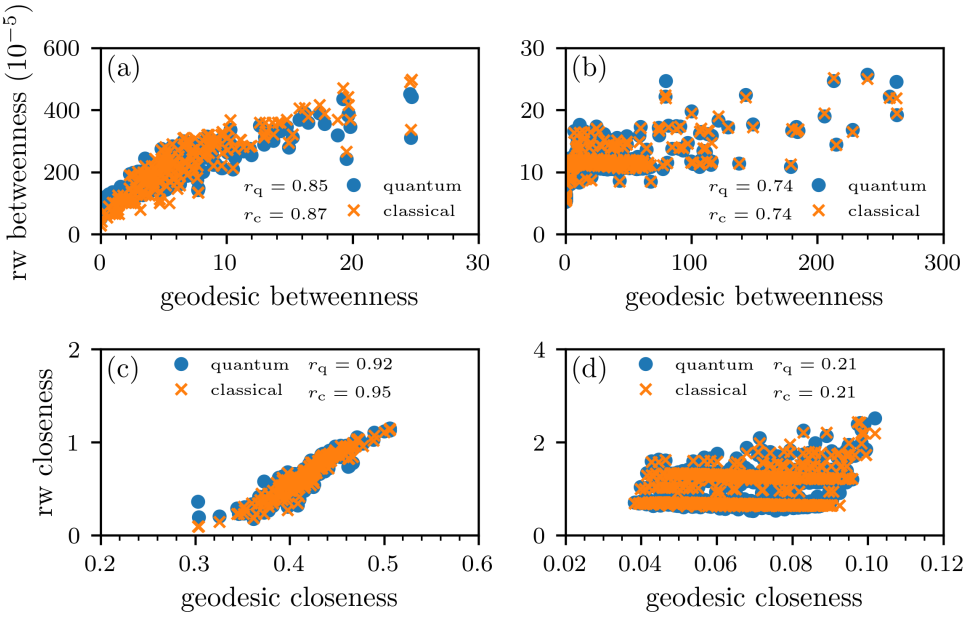

FIG. 8. Correlations between random-walk and geodesic centralities on empirical multilayer networks. *We show the correlations between random-walk (rw) and geodesic betweenness and closeness on two empirical multilayer networks. We use* r_c *and* r_q *to denote the numerical values of the Pearson correlation coefficients for classical and quantum centralities, respectively. We denote the classical and quantum random-walk centralities using orange crosses and blue disks, respectively. In the resolvent (see Table* 1*), we set* $s = 0.01$. (a,c) *The Lazega Law Firm network, which has* 71 *nodes and* 2571 *edges.* (b,d) *A multilayer network of the London metropolitan ("Tube") network with* 369 *nodes and* 441 *edges. It has three edge types, which encode connections in the three layers (Underground, Overground, and Docklands Light Railway) of London metro stations. In both of these multilayer networks, interlayer edges connect each node-layer with its counterpart in the other layer. As the initial condition for each calculation, we use a uniform distribution over all node-layers.*

There are various interesting ways to build on our work. One worthwhile direction is to develop multilayer extensions of generalized versions of PageRank [15] with various teleportation strategies and to compare classical and quantum versions of these generalizations. One can use and adapt existing multilayer generalizations, such as multilayer personalized PageRank [22] (in which the teleportation strategy depends on the initial location of a random walker) and multilayer versions of PageRank that include both node teleportation and layer teleportation [56]. One can also generalize other versions of PageRank, such as ones with "smart teleportation" [26], to multilayer networks and then compare classical and quantum versions of such generalizations. Another important research direction is to consider more general types of quantum states. We considered pure quantum states in our derivations and numerical experiments, and it will be interesting to explore the effects of entangled and mixed states on the node-occupation properties of quantum walks. One can also use the framework of quantum stochastic walks (QSWs) [59, 60] to interpolate between classical and quantum walks, and it is worthwhile to study QSWs on multilayer networks.

Acknowledgments. We thank Sascha Wald for helpful discussions.

Copyright © by SIAM. Unauthorized reproduction of this article is prohibited.

Downloaded 01/30/25 to 108.147.175.114 . Redistribution subject to SIAM license or copyright; see https://epubs.siam.org/terms-privacy

Downloaded 01/30/25 to 108.147.175.114 . Redistribution subject to SIAM license or copyright; see https://epubs.siam.org/terms-privacy

REFERENCES

[1] *Lazega Law Firm Network*, https://networks.skewed.de/net/law_firm, 2020.

[2] *London Transport Network*, https://networks.skewed.de/net/london_transport, 2020.

[3] A. Aleta and Y. Moreno, *Multilayer networks in a nutshell*, Annu. Rev. Condens. Matter Phys., 10 (2019), pp. 45–62.

[4] E. C. Baek, M. A. Porter, and C. Parkinson, *Social network analysis for social neuroscientists*, Soc. Cogn. Affect. Neurosc., 16 (2021), pp. 883–901.

[5] S. D. Berry and J. B. Wang, *Quantum-walk-based search and centrality*, Phys. A, 82 (2010), 042333.

[6] L. Böttcher, *GitLab Repository*, https://gitlab.com/ComputationalScience/ctqw_centrality, 2020.

[7] D. Bouwmeester, I. Marzoli, G. P. Karman, W. Schleich, and J. Woerdman, *Optical Galton board*, Phys. Rev. A, 61 (1999), 013410.

[8] S. Chakraborty, L. Novo, A. Ambainis, and Y. Omar, *Spatial search by quantum walk is optimal for almost all graphs*, Phys. Rev. Lett., 116 (2016), 100501.

[9] A. M. Childs and J. Goldstone, *Spatial search by quantum walk*, Phys. Rev. A, 70 (2004), 022314.

[10] M. De Domenico, A. Solé-Ribalta, E. Cozzo, M. Kivelä, Y. Moreno, M. A. Porter, S. Gómez, and A. Arenas, *Mathematical formulation of multilayer networks*, Phys. Rev. X, 3 (2013), 041022.

[11] M. De Domenico, A. Solé-Ribalta, S. Gómez, and A. Arenas, *Navigability of interconnected networks under random failures*, Proc. Natl. Acad. Sci. USA, 111 (2014), pp. 8351–8356.

[12] M. De Domenico, A. Solé-Ribalta, E. Omodei, S. Gómez, and A. Arenas, *Ranking in interconnected multilayer networks reveals versatile nodes*, Nat. Commun., 6 (2015), 6868.

[13] B. Do, M. L. Stohler, S. Balasubramanian, D. S. Elliott, C. Eash, E. Fischbach, M. A. Fischbach, A. Mills, and B. Zwickl, *Experimental realization of a quantum quincunx by use of linear optical elements*, J. Opt. Soc. Amer. B, 22 (2005), pp. 499–504.

[14] M. Faccin, T. Johnson, J. Biamonte, S. Kais, and P. Migdał, *Degree distribution in quantum walks on complex networks*, Phys. Rev. X, 3 (2013), 041007.

[15] D. F. Gleich, *PageRank beyond the Web*, SIAM Rev., 57 (2015), pp. 321–363.

[16] S. Gomez, A. Diaz-Guilera, J. Gomez-Gardenes, C. J. Perez-Vicente, Y. Moreno, and A. Arenas, *Diffusion dynamics on multiplex networks*, Phys. Rev. Lett., 110 (2013), 028701.

[17] L. K. Grover, *A fast quantum mechanical algorithm for database search*, in Proceedings of the Twenty-Eighth Annual ACM Symposium on Theory of Computing, 1996, pp. 212–219.

[18] L. K. Grover, *Quantum mechanics helps in searching for a needle in a haystack*, Phys. Rev. Lett., 79 (1997), pp. 325–328.

[19] J. A. Izaac, X. Zhan, Z. Bian, K. Wang, J. Li, J. B. Wang, and P. Xue, *Centrality measure based on continuous-time quantum walks and experimental realization*, Phys. Rev. A, 95 (2017), 032318.

[20] K. A. Jacobsen and J. H. Tien, *A generalized inverse for graphs with absorption*, Linear Algebra Appl., 537 (2018), pp. 118–147.

[21] J. Janmark, D. A. Meyer, and T. G. Wong, *Global symmetry is unnecessary for fast quantum search*, Phys. Rev. Lett., 112 (2014), 210502.

[22] L. G. S. Jeub, M. W. Mahoney, P. J. Mucha, and M. A. Porter, *A local perspective on community structure in multilayer networks*, Netw. Sci., 5 (2017), pp. 44–163.

[23] M. Karski, L. Förster, J.-M. Choi, A. Steffen, W. Alt, D. Meschede, and A. Widera, *Quantum walk in position space with single optically trapped atoms*, Science, 325 (2009), pp. 174–177.

[24] M. Kivelä, A. Arenas, M. Barthelemy, J. P. Gleeson, Y. Moreno, and M. A. Porter, *Multilayer networks*, J. Complex Netw., 2 (2014), pp. 203–271.

[25] T. G. Kolda and B. W. Bader, *Tensor decompositions and applications*, SIAM Rev., 51 (2009), pp. 455–500.

[26] R. Lambiotte and M. Rosvall, *Ranking and clustering of nodes in networks with smart teleportation*, Phys. Rev. E, 85 (2012), 056107.

[27] E. Lazega, *The Collegial Phenomenon: The Social Mechanisms of Cooperation among Peers in a Corporate Law Partnership*, Oxford University Press, Oxford, 2001.

[28] T. Loke, J. Tang, J. Rodriguez, M. Small, and J. B. Wang, *Comparing classical and quantum PageRanks*, Quantum Inf. Process., 16 (2017), 25.

[29] W. Luo, W. P. Tay, and M. Leng, *Identifying infection sources and regions in large networks*, IEEE Trans. Signal Process., 61 (2013), pp. 2850–2865.

Copyright © by SIAM. Unauthorized reproduction of this article is prohibited.

[30] A. Mahasinghe, J. Wang, and J. Wijerathna, *Quantum walk-based search and symmetries in graphs*, J. Phys. A Math. Theoret., 47 (2014), 505301.
[31] N. Masuda, M. A. Porter, and R. Lambiotte, *Random walks and diffusion on networks*, Phys. Rep., 716 (2017), pp. 1–58.
[32] O. Mülken and A. Blumen, *Continuous-time quantum walks: Models for coherent transport on complex networks*, Phys. Rep., 502 (2011), pp. 37–87.
[33] O. Mülken, A. Blumen, T. Amthor, C. Giese, M. Reetz-Lamour, and M. Weidemüller, *Survival probabilities in coherent exciton transfer with trapping*, Phys. Rev. Lett., 99 (2007), 090601.
[34] S. Nauer, L. Böttcher, and M. A. Porter, *Random-graph models and characterization of granular networks*, J. Complex Netw., 8 (2020), cnz037.
[35] M. E. J. Newman, *A measure of betweenness centrality based on random walks*, Soc. Netw., 27 (2005), pp. 39–54.
[36] M. E. J. Newman, *Networks*, 2nd ed., Oxford University Press, Oxford, 2018.
[37] J. D. Noh and H. Rieger, *Random walks on complex networks*, Phys. Rev. Lett., 92 (2004), 118701.
[38] J. R. Norris, *Markov Chains*, Cambridge University Press, Cambridge, 1998.
[39] L. Papadopoulos, M. A. Porter, K. E. Daniels, and D. S. Bassett, *Network analysis of particles and grains*, J. Complex Netw., 6 (2018), pp. 485–565.
[40] G. D. Paparo and M. Martin-Delgado, *Google in a quantum network*, Sci. Rep., 2 (2012), 444.
[41] A. Pazy, *Semigroups of Linear Operators and Applications to Partial Differential Equations*, Vol. 44, Springer-Verlag, Berlin, 2012.
[42] H. B. Perets, Y. Lahini, F. Pozzi, M. Sorel, R. Morandotti, and Y. Silberberg, *Realization of quantum walks with negligible decoherence in waveguide lattices*, Phys. Rev. Lett., 100 (2008), 170506.
[43] P. Philipp, L. Tarrataca, and S. Boettcher, *Continuous-time quantum search on balanced trees*, Phys. Rev. A, 93 (2016), 032305.
[44] M. A. Porter, *WHAT is ... a multilayer network?*, Notices Amer. Math. Soc., 65 (2018), pp. 1419–1423.
[45] R. Portugal, *Quantum Walks and Search Algorithms*, Springer-Verlag, Berlin, 2013.
[46] L. Rossi, A. Torsello, and E. R. Hancock, *Node centrality for continuous-time quantum walks*, in Joint IAPR International Workshops on Statistical Techniques in Pattern Recognition (SPR) and Structural and Syntactic Pattern Recognition (SSPR), Springer-Verlag, Berlin, 2014, pp. 103–112.
[47] C. A. Ryan, M. Laforest, J.-C. Boileau, and R. Laflamme, *Experimental implementation of a discrete-time quantum random walk on an NMR quantum-information processor*, Phys. Rev. A, 72 (2005), 062317.
[48] E. Sánchez-Burillo, J. Duch, J. Gómez-Gardenes, and D. Zueco, *Quantum navigation and ranking in complex networks*, Sci. Rep., 2 (2012), 605.
[49] H. Schmitz, R. Matjeschk, C. Schneider, J. Glueckert, M. Enderlein, T. Huber, and T. Schaetz, *Quantum walk of a trapped ion in phase space*, Phys. Rev. Lett., 103 (2009), 090504.
[50] A. Schreiber, K. N. Cassemiro, V. Potoček, A. Gábris, P. J. Mosley, E. Andersson, I. Jex, and C. Silberhorn, *Photons walking the line: A quantum walk with adjustable coin operations*, Phys. Rev. Lett., 104 (2010), 050502.
[51] D. Shah and T. Zaman, *Rumors in a network: Who's the culprit?*, IEEE Trans. Inform. Theory, 57 (2011), pp. 5163–5181.
[52] L. Solá, M. Romance, R. Criado, J. Flores, A. García del Amo, and S. Boccaletti, *Eigenvector centrality of nodes in multiplex networks*, Chaos, 23 (2013), 033131.
[53] A. Solé-Ribalta, M. De Domenico, S. Gómez, and A. Arenas, *Random walk centrality in interconnected multilayer networks*, Phys. D, 323 (2016), pp. 73–79.
[54] A. Solé-Ribalta, M. De Domenico, N. E. Kouvaris, A. Diaz-Guilera, S. Gomez, and A. Arenas, *Spectral properties of the Laplacian of multiplex networks*, Phys. Rev. E, 88 (2013), 032807.
[55] H. Tang, R. Shi, T.-S. He, Y.-Y. Zhu, T.-Y. Wang, M. Lee, and X.-M. Jin, *TensorFlow solver for quantum PageRank in large-scale networks*, Sci. Bull., 66 (2021), pp. 120–126.
[56] D. Taylor, M. A. Porter, and P. J. Mucha, *Tunable eigenvector-based centralities for multiplex and temporal networks*, Multiscale Model. Simul., 19 (2021), pp. 113–147.
[57] G. Teschl, *Mathematical Methods in Quantum Mechanics*, American Mathematical Society, Providence, RI, 2009.
[58] B. Thaller, *Advanced Visual Quantum Mechanics*, Springer-Verlag, Berlin, 2005.

Downloaded 01/30/25 to 108.147.175.114 . Redistribution subject to SIAM license or copyright; see https://epubs.siam.org/terms-privacy

Copyright © by SIAM. Unauthorized reproduction of this article is prohibited.

[59] S. Wald and L. Böttcher, *From classical to quantum walks with stochastic resetting on networks*, Phys. Rev. E, 103 (2021), 012122.
[60] J. D. Whitfield, C. A. Rodríguez-Rosario, and A. Aspuru-Guzik, *Quantum stochastic walks: A generalization of classical random walks and quantum walks*, Phys. Rev. A, 81 (2010), 022323.
[61] T. G. Wong, L. Tarrataca, and N. Nahimov, *Laplacian versus adjacency matrix in quantum walk search*, Quantum Inf. Process., 15 (2016), pp. 4029–4048.
[62] S. Yalouz and V. Pouthier, *Continuous-time quantum walk on an extended star graph: Trapping and superradiance transition*, Phys. Rev. E, 97 (2018), 022304.
[63] F. Zähringer, G. Kirchmair, R. Gerritsma, E. Solano, R. Blatt, and C. F. Roos, *Realization of a quantum walk with one and two trapped ions*, Phys. Rev. Lett., 104 (2010), 100503.

Downloaded 01/30/25 to 108.147.175.114 . Redistribution subject to SIAM license or copyright; see https://epubs.siam.org/terms-privacy

Copyright © by SIAM. Unauthorized reproduction of this article is prohibited.